université paris sud
INSTITUT DE PHYSIQUE NUCLEAIRE
BP N° 1 91406 - ORSAY TEL. 941.51.10
laboratoire associé à l'IN2P3

FR 8002091

SINGLE-PARTICLE AND CORE-EXCITED STATES IN ^{49}Sc I THE $^{48}Ca(^{3}He,d)^{49}Sc$ REACTION

S. FORTIER, E. HOURANI*
and
J.M. MAISON

Institut de Physique Nucléaire, BP N°1
91400 ORSAY, FRANCE

IPNO-PhN-80-09

SINGLE-PARTICLE AND CORE-EXCITED STATES IN ^{49}Sc

I THE $^{48}Ca(^{3}He,d)^{49}Sc$ REACTION

S. FORTIER, E. HOURANI* AND J.M. MAISON

Institut de Physique Nucléaire, B.P. N°1, 91400 ORSAY, FRANCE

Abstract : The $^{48}Ca(^{3}He,d)^{49}Sc$ reaction has been studied at 25 MeV incident energy. Angular distributions have been measured from 5° to 40° using a split pole spectrometer, for about 160 levels located up to 18 MeV excitation energy. A local zero range DWBA analysis has been carried out, using Gamow functions as form factors in the case of unbound states; ℓ assignments and spectroscopic factors are obtained for a large number of levels, most of them previously unknown. The summed experimental spectroscopic strengths for the $T_<$, $\ell = 1$ and $\ell = 3$ levels are in good agreement with the shell-model sum rule limits for 1f-2p proton states, and their energy centroids have been determined. The $1g_{9/2}$ strength in ^{49}Sc is strongly fragmented : about 27 % of the $T_<$ strength is carried by twenty three levels located between 6.5 and 13.5 MeV. Spectroscopic factors for analog states are compared with those from previous (p,p), (^{3}He,dp) and (d,p) experiments.

NUCLEAR REACTIONS $^{48}Ca(^{3}He,d)$, E = 25 MeV; measured $\sigma(E_d,\theta)$. ^{49}Sc deduced levels, ℓ, S, analog states. DWBA analysis. Enriched target.

* Permanent address : Lebanese University, Faculty of Sciences, Hadat-Beyrouth, Lebanon.

I. Introduction.

Spectroscopic data about low-lying levels in ^{49}Sc have been obtained from γ-ray work and one-proton transfer reactions[1]. In addition, isobaric analog states have been extensively studied through proton-induced resonant reactions[1] and the (^3He,dp) reaction[2]. However, in spite of the large theoretical interest for this nucleus, close to the magic ^{48}Ca nucleus, available experimental information was not so large as for many other $f_{7/2}$ nuclei. In particular, due to the lack of data about levels in the 7 to 11.5 MeV energy region, the location of centroids for the $f_{5/2}$, $p_{3/2}$ and $p_{1/2}$ strengths in ^{49}Sc could not be determined and very little was known about the $g_{9/2}$ strength. In the other hand, high spin states (with $J > 9/2$) were up to now experimentally unknown in ^{49}Sc. Such high spin states in ^{49}Sc can in fact be expected above 3.7 MeV excitation energy, as resulting from the coupling of one $f_{7/2}$ proton with the low-lying excited states of ^{48}Ca.

In order to study these two points -the fragmentation of single- particle strengths in ^{49}Sc and the existence of low-lying core -excited states with a high spin value- a comparative investigation of the $^{48}Ca(^3He,d)^{49}Sc$ and $^{48}Ca(\alpha,t)^{49}Sc$ reactions has been done. In the next paper (further called II) we shall present the results of the (α,t) reaction, comparing them with those obtained in the (^3He,d) reaction. The present paper reports the results of the $^{48}Ca(^3He,d)^{49}Sc$ reaction at 25 MeV, obtained in the 0-18 MeV excitation energy range, and is mainly devoted to the study of the fragmentation of the single particle states in ^{49}Sc.

2. Experimental procedure

The $^{48}Ca(^{3}He,d)^{49}Sc$ reaction was investigated at 25 MeV incident energy with the Orsay MP Tandem. The deuterons were detected with eight 1000 μm thick position sensitive Si detectors placed in the focal plane of a split-pole spectrometer. They were discriminated from other light particles with the same Bρ value by considering the energy loss in the detectors. The experiment was carried out in two distinct runs : the 0-12 MeV excitation energy range was studied using a 250 $\mu g/cm^2$ thick ^{48}Ca target, whereas the target thickness for studying the high energy (11-17 MeV) part was about 350 $\mu g/cm^2$. The isotopic enrichment in ^{48}Ca was 97.2 %. The overall energy resolution was about 25-30 keV. Angular distributions were measured in 5° steps from 5° to 40° lab angle. Two successive exposures at different magnetic fields were necessary at each angle in order to cover the spacings between adjacent detectors in the focal plane. The whole deuteron spectra presented in fig. 1 were obtained by juxtaposition of both sets of individual spectra for each detector, overlapping each other in a range of 100 to 300 keV.

About 150 levels or groups of levels in ^{49}Sc have been observed in the present experiment. Their excitation energies are reported in table 1. They were deduced from a calibration of the radius versus the channel number, obtained in a preliminary experiment. For the low-energy part (E_x < 12 MeV), this calibration was done by observing the peak positions for the four lowest states in ^{49}Sc with accurately known excitation energies[1], at various values of the magnetic field. The accuracy is estimated to be about 8 keV below 8 MeV and 20 keV between 8 and 12 MeV. The calibration for the high energy part was deduced from the positions of α-peaks from the $^{58}Ni(^{3}He,\alpha)^{57}Ni$ reaction at 25 MeV, obtained for various values of the magnetic fields.

Absolute cross sections were obtained by comparing the 25 MeV ^{3}He scattering data at 10° and 12° (lab) with optical model predictions. At these

forward angles, theoretical elastic cross sections are very close to the Rutherford predictions, and are almost independant of relatively wide variations of the optical parameters. Independantly of statistics, this procedure is estimated to give an overall accuracy of about 15 % for the determination of absolute cross sections.

3. Distorted wave analysis

3.1 - DWBA calculations.

The distorted wave analysis for both bound and unbound states was performed in the same manner as in our previous (^{3}He,d) experiments on (f-p) shell nuclei[3-6]. Zero-range DWBA calculations for bound states were performed with the code DWUCK [7]. The geometrical parameters used for the determination of the bound states form factors are listed in table 2, together with the optical potential parameters for the ^{3}He and deuteron channels. These optical potentials[8,9] extracted from a systematic analysis of elastic scattering data, give a rather good agreement between theoretical and experimental (^{3}He,d) angular distribution, as it is shown in figs 2-4.

The proton form factors for stripping to unbound states in ^{49}Sc (above 9.6 MeV excitation energy) were calculated using Gamow functions $\tilde{g}_{\ell j}(r)$ following the method of Coker and Hoffmann[10]. Gamow functions are solutions of the radial Schrödinger equation for the complex energy $(E_R - \frac{1}{2} i \Gamma_{sp})$ of the resonant state (E_R is the energy of the resonance in the c.m. system and $\Gamma_{s.p.}$ is the single-particle width). Numerical computation of form factors was performed using the program GAMOW)[10]. For a given (l,j) transition, the well depth of the proton optical potential (with the same geometrical parameters as for bound states) was adjusted in order to obtain the correct energy E_R of the resonant state and the single-particle width $\Gamma_{s.p.}$. These complex form factors were then introduced in the program VENUS[11] and the DWBA calculations were performed in the same conditions as for bound states. As it is physically expected, theoretical cross sections for various (l,j) transfers are observed to vary continuously across the zero binding energy.

3.2 - Angular distributions and spectroscopic strengths.

Experimental angular distributions have been compared to DWBA predictions, leading to ℓ-assignments and determination of spectroscopic strengths. Some examples are displayed in figs 2-4 for various transfered angular momenta. The variation of the shapes of angular distributions with excitation energy is well reproduced by DWBA calculations and ℓ-assignments can generally be made without ambiguity. They are reported in table 1 for about one hundred levels. However, above 10 MeV, $\ell = 3$ and $\ell = 4$ transitions cannot be surely discriminated, because of similar shapes of angular distributions (cf. fig. 4). As it will be shown in §4, these transitions are probably $\ell = 4$ for the major part, this assertion being based on a sum rule analysis and shell model considerations.

Some angular distributions can only be reproduced by the addition of two different ℓ-transfers. This is for example the case for the peak at 7.06 MeV, which is a doublet of closely spaced $\ell = 1$ and $\ell = 4$ levels, and can be identified with the level observed at about 7.12 MeV and tentatively assigned $\ell = 4$ in (^{3}He,d) and (α,t) reactions[12]. Similarly, a group of angular distributions between 11.7 and 12.3 MeV, with mainly an $\ell = 1$ character, are better reproduced by a mixing of $(\ell = 1) + (\ell = 3)$ or $(\ell = 1) + (\ell = 4)$ transitions, but the proportion of each transition could not be given without a large uncertainty.

Spectroscopic factors were deduced from the theoretical cross sections, $\sigma_{DW}^{\ell j}$, by means of the expression

$$(d\sigma/d\Omega)_{exp} = N\ C^2S\ \sigma_{DW}^{\ell j} \qquad (1)$$

where N is the normalization factor, taken equal to the usual value of 4.42. The spectroscopic strengths $(2J+1)\ C^2S$ extracted from this analysis are reported in table 1. When the spin value was previously unknown, the determination of spectroscopic strengths was done by assuming a definite value based on the transfered angular momentum and shell model considerations.

This assumed spin value is indicated in table 1, as the first of the two possible values. The $\ell = 4$ transitions are interpreted as a stripping to the $g_{9/2}$ subshell. The $\ell = 0$ and $\ell = 2$ transitions below 6 MeV excitation energy are assumed to be due to the stripping to the inner 2s-1d shell, whereas a $2d_{5/2}$ transfer is assumed for the higher-lying $\ell = 2$ transitions. Spectroscopic strengths determined assuming $j = \ell - 1/2$ are higher than for $j = \ell + 1/2$ with a ratio of about 1.15, 1.33 and 1.50 for transfered angular momentum of 1, 2 and 3, respectively.

The spectroscopic strengths deduced from this analysis are compared in table 3 with those from the previous (^{3}He,d) experiments[1]. Previous results only concern the strongest transitions and are generally in good agreement with the present data, if one takes into account the 20 % estimated uncertainty on spectroscopic factors, due to the DWBA approximations.

3.3 - "Non-stripping" levels.

A few low-lying levels, excited with a low cross-section, display angular distributions which are not reproduced by the DWBA calculations. They are labelled "ns" in table 1, in order to point out that they are excited through a non stripping mechanism. They will be discussed in paper (II).

4. Results and discussion

4.1 - Isobaric analog states in ^{49}Sc.

A large amount of data about analog states has been obtained from the study of proton induced resonant reactions[1]. In the other hand, the study of the proton decay of analog states through the ^{48}Ca(^{3}He,dp) sequential reaction has given another source of information on spectroscopic factors relative to

the ground and excited states of ^{48}Ca[2]. In the present work, the identification of analog states is based on their measured excitation energy and transfered angular momentum. The high-energy part of the $^{48}Ca(^3He,d)$ spectrum (cf. fig. 1 bis) is largely dominated by analog states (labelled $T_>$), in particular the $p_{3/2}$ analog of the ^{49}Ca ground state and the $f_{5/2}$ and $g_{9/2}$ analog states above 15 MeV excitation energy. Three levels or groups of levels at about 13.5 MeV have a dominant $\ell = 1$ angular distribution and are probably components of the $p_{1/2}$ analog state, observed in elastic scattering experiments with a natural width of 200 keV. Finally, a deuteron group corresponding to a ^{49}Sc level is observed at about 18 MeV excitation energy. An identification with the $5/2^+$ resonance at 18.15 MeV (réf. 19), proposed to be the analog state of a ^{49}Ca level at 6.7 MeV, should only be tentative because its angular distribution is not characteristic of an $\ell = 2$ transfer.

The present results about analog states in ^{49}Sc are summarized in table 4. The spectroscopic factors deduced from the DWBA analysis of the $(^3He,d)$ reaction can be compared with those found for the parent states in ^{49}Ca, obtained from the study of the $^{48}Ca(d,p)^{49}Ca$ reaction[20]. These values should be theoretically equal. Experimentally, they agree within 25 % for the $p_{3/2}$, $p_{1/2}$ and $g_{9/2}$ states, whereas a 40 % difference is found for the $lf_{5/2}$ states. These slight differences are of the same order as those found in the previous $(^3He,d)$ studies of analog states in the $lf_{7/2}$ region[3-6]; they can be explained by considering the dependance of DWBA cross sections on different optical potentials and geometrical parameters of the proton well, used in the form factor calculation.

The $(^3He,d)$ spectroscopic factors for analog states are also compared in table 4 with those deduced from (p,p) and $(^3He,dp)$ experiments[2, 18, 19]. Here again, the agreement between the results can be considered as rather good, considering : i) the 20 % estimated uncertainty on DWBA cross sections; ii) an uncertainty of about the some order for the single particle width Γ_{sp}

used in the determination of the S value in the (p,p) and (^{3}He,dp) work (cf. table 4), which is not included in the quoted errors.

4.2 - Distribution of single particle strengths in ^{49}Sc.

For all different ℓ-transfers observed in the present study of the ^{48}Ca(^{3}He,d)^{49}Sc reaction, the distribution of spectroscopic strengths with respect to excitation energy is displayed in fig. 5. Here a $1g_{9/2}$ transfer is definitely assumed for levels above 11 MeV, with an angular distribution compatible with both $\ell = 3$ and $\ell = 4$ assignments. Such an assertion is based on the exhausted shell-model sum-rule for $f_{7/2}$ and $f_{5/2}$ transitions below this excitation energy. This is shown in Table 5, where the sums of experimental spectroscopic strengths for $\ell = 1$, $\ell = 3$ and $\ell = 4$ transitions are compared with the sum-rule limits for both $T_>$ and $T_<$ states (where $T_<$ is the isospin value of the ^{49}Sc ground state). We now discuss the fragmentation of the $T_<$ one proton strengths in ^{49}Sc.

- $\ell = 3$ transitions: In addition to the $f_{7/2}$ ground state, spin 7/2 was previously assigned to only two levels (see table 1). The sum-rule analysis in table 5 shows that more than 90 % of the $f_{7/2}$ strength is concentrated in these three levels. In the other hand, the sum of spectroscopic strengths for $f_{7/2}$ and $f_{5/2}$ transitions agree within 5 % with the shell-model predictions, indicating that the main fragments of the $f_{7/2}$ and $f_{5/2}$ one-proton states are observed in the present experiment. The energy centroids of the $f_{7/2}$ and $f_{5/2}$ states, calculated from the relation $\overline{E}_p = \sum_i (2J+1)C^2S_i E_i / \sum_i (2J+1)C^2S_i$, are also given in table 5.

- $\ell = 1$ transitions : The summed spectroscopic strengths for $\ell = 1$ transitions are also in good agreement with the shell-model sum-rule. In order to get an accurate determination of the $p_{3/2}$-$p_{1/2}$ energy splitting in ^{49}Sc, it would be necessary to perform additionnal spin measurement : as it is shown in table 5, the previously known $3/2^-$ levels only share 58 % of the total $p_{3/2}$

strength; therefore a part of the other $\ell = 1$ levels necessarily have spin 3/2. In table 5, it is arbitrarily assumed that all $\ell = 1$ levels below 8 MeV, with unknown J^{π}, have spin 3/2 and thus exhaust the total $p_{3/2}$ sum rule : in this case, the $p_{3/2} - p_{1/2}$ splitting would be approximately 4 MeV.

- $\ell = 4$ transitions : Only one $\ell = 4$ level in ^{49}Sc was known from previous proton stripping experiments[12]. In addition to the 7.06 MeV level, 22 other $\ell = 4$, $T_<$ transitions are observed in the present reaction, between 6.5 and 13.5 MeV excitation energy with an energy centroid at 10.1 MeV. However, the sum of experimental spectroscopic strengths is only 27 % of the $g_{9/2}$ sum rule limit. The missing $g_{9/2}$ strength is probably shared between a large number of very weak fragments, located in the continuum and undetectable in the present experiment.

- $\ell = 0$ and $\ell = 2$ transitions : low lying transitions can be interpreted as a stripping to the inner 2s-1d shell in ^{48}Ca, as the components of the $3s_{1/2}$ and $2d_{5/2}$ states are expected to lie at higher energy than the $g_{9/2}$ states, because of shell-model considerations. Ten weak $\ell = 2$ transitions are observed between 2.4 and 11.4 MeV. In addition to the known $\frac{1}{2}^+$ level at 2.23 MeV, two other $\ell = 0$ transitions at 3.99 and 6.91 MeV are observed for the first time. The summed spectroscopic strength for $\ell = 0$ transitions in the ^{48}Ca(^{3}He,d)^{49}Sc reaction is only 0.07, once more confirming the good closure of the ^{48}Ca core : the deduced occupancy number for the $2s_{1/2}$ subshell is about 97 %.

5. Conclusion

The spectroscopic information about single-particle states in ^{49}Sc has been greatly increased by the present results of the ^{48}Ca(^{3}He,d)^{49}Sc reaction, with ℓ-assignment and determination of spectroscopic strengths for about a

hundred levels up to 18 MeV excitation energy. In particular, the location and fragmentation of the $1g_{9/2}$ strength in ^{49}Sc has been evidenced for the first time.

In the next paper (II), we report a study of the $^{48}Ca(\alpha,t)^{49}Sc$ reaction, where a special attention is given to the possible two-step excitation of core excited states in ^{49}Sc. It is worth noticing that a standard DWBA analysis successfully reproduces the largest part of the present (^3He,d) angular distributions, indicating that the (^3He,d) reactions at 25 MeV incident energy is well dominated by a direct stripping process.

We acknowledge Dr S. Galès for his assistance in the early stage of the experiment and for fruitful discussions. We wish to thank J.C. Artiges and P. Cohen for their help in the electronic set-up and the operating crew of the Orsay Tandem for the efficient running of the accelerator. One of us (E.H.) acknowledges the partial financial support of the CNRS of Lebanon.

References

1) M.L. Halbert, Nuclear Data Sheets 24 (1978) 175 and refs therein.

2) S. Gales, S. Fortier, H. Laurent, J.M. Maison and J.P. Schapira, Phys. Lett. 56 B (1975) 41.

3) S. Gales, S. Fortier, H. Laurent, J.M. Maison and J.P. Schapira, Nucl. Phys. A259 (1976) 189.

4) S. Gales, S. Fortier, H. Laurent, J.M. Maison and J.P. Schapira, Nucl. Phys. A 265 (1976) 213.

5) S. Gales, S. Fortier, H. Laurent, J.M. Maison and J.P. Schapira, Nucl. Phys. A 268 (1976) 257.

6) S. Fortier, J.M. Maison, S. Gales, H. Laurent and J.P. Schapira, Nucl. Phys. A 288 (1977) 82.

7) P.D. Kunz, University of Colorado, report COO-535-606.

8) F.D. Becchetti, Jr. and G.W. Greenless, in "Polarization Phenomene in Nuclear Reactions", ed. H.H. Barshall and W. Haeberli (University of Wisconsin Press, Madison WS, 1971) p 682.

9) C.M. Perey and F.G. Perey, Phys. Rev. 132 (1963) 755.

10) W.R. Coker and G.W. Hoffmann, Z. Phys. 263 (1973) 179.

11) T. Tamura, W.R. Coker and F.J. Rejbicki, Comp. Phys. Comm. 2 (1971) 34.

12) G. Bruge, H. Faraggi, Ha Duc Long et P. Roussel, rapport CEA-N- 1232 (1970) 124.

13) J.R. Erskine, A. Marinov and J.P. Schiffer, Phys. Rev. 142 (1966) 633.

14) R.M. Britton and D.L. Watson, Nucl. Phys. A272 (1976) 91.

15) D.D. Armstrong and A.G. Blair, Phys. Rev. 140 (1965) B 1226.

16) K.W. Kemper, A.F. Zeller and T.R. Ophel, J. Phys. G4 (1978) L 17.

17) W.D. Metz, W.D. Callender and C.K. Backelman, Phys. Rev. C12 (1975) 827.

18) K.W. Jones et al., Phys. Rev. 145 (1966) 894.

19) E. Navon et al., Nucl. Phys. A329 (1979) 127.

Table 1 : Levels observed in the $^{48}Ca(^{3}He,d)^{49}Sc$ reaction at 25 MeV

Peak N°	Ex [a] (MeV)	Ex [b] (MeV±keV)	ℓ [a]	J^{π}	$(2J+1)C^2S$	$(d\sigma/d\Omega)_{CM}$ at 5° lab (mb/sr)
1	0		3	$\frac{7}{2}^{-}$ b)	6.72	0.98
2	2.229	2.229 (0.3)	0	$\frac{1}{2}^{+}$ b)	0.03	0.53
3	2.372	2.372 (0.4)	2	$\frac{3}{2}^{+}$ b)	0.05	0.035
4	3.084	3.084 (0.1)	1	$\frac{3}{2}^{-}$ b)	2.08	24.2
5	3.517	3.517 (5)	ns			0.035
6	3.755		2	$(\frac{3}{2}, \frac{5}{2})^{+}$	0.01	0.011
7	3.809	3.809 (5)	3	$\frac{7}{2}^{-}$ c)	0.53	0.23
8	3.921	3.923 (10)	ns			0.018
9	3.992	3.991 (9)	0	$\frac{1}{2}^{+}$	0.02	0.43
10	4.072	4.072 (1)	3	$\frac{5}{2}^{-}$ b)	0.98	0.45
11	4.220		ns			0.010
12	4.285		ns			0.009
13	4.333	4.341	3	$(\frac{5}{2}, \frac{7}{2})^{-}$	0.44	0.22
14	4.495	4.495 (2)	1	$\frac{1}{2}^{-}$ c)	1.04	14.2
15	4.579		1	$(\frac{1}{2}, \frac{3}{2})^{-}$	0.02	0.28
16	4.711		1	$(\frac{1}{2}, \frac{3}{2})^{-}$	0.01	0.14
17	4.738	4.738 (2)	3	$\frac{5}{2}^{-}$ b)	0.70	0.47
18	4.810		3	$(\frac{5}{2}, \frac{7}{2})^{-}$	0.03	0.013
19	4.948		(1)	$(\frac{1}{2}, \frac{3}{2})^{-}$	0.001	0.016
20	5.015	5.008 (11)	1	$(\frac{1}{2}, \frac{3}{2})^{-}$	0.19	2.3

Peak N°	Ex [a] (MeV)	Ex [b] (MeV±keV)	ℓ [a]	J^π	$(2J+1)C^2S$	$(d\sigma/d\Omega)_{CM}$ at 5° lab (mb/sr)
21	5.077	5.080 (10)	3	$(\frac{5}{2}, \frac{7}{2})^-$	1.99	1.5
22	5.230		2	$(\frac{3}{2}, \frac{5}{2})^+$	0.02	0.040
23	5.380	5.376 (5)	3	$(\frac{5}{2}, \frac{7}{2})^-$	0.81	0.60
24	5.438		ns			0.058
25	5.578		2	$(\frac{3}{2}, \frac{5}{2})^+$	0.05	0.11
26	5.663	5.655 (9)	1	$(\frac{1}{2}, \frac{3}{2})^-$	0.39	5.5
27	5.815	5.811 (11)	1	$(\frac{1}{2}, \frac{3}{2})^-$	0.08	1.2
28	5.845					0.20
29	6.000					0.15
30	6.014					
31	6.069		(2)	$(\frac{3}{2}, \frac{5}{2})^+$	0.02	0.038
32	6.180		2	$(\frac{3}{2}, \frac{5}{2})^+$	0.08	0.20
33	6.250		ns			0.12
34	6.266					
35	6.307	6.306 (3)	ns	$(\frac{5}{2})^-$ [b]		0.080
36	6.412	6.416 (4)	3	$\frac{7}{2}^-$ [b]	0.14	0.25
37 [d]	6.527	6.555 (12)	1	$(\frac{1}{2}, \frac{3}{2})^-$	0.03	0.71
			4	$(\frac{9}{2}, \frac{7}{2})^+$	0.20	
38	6.685					-
39	6.717	6.728 (3)	1	$\frac{3}{2}^-$	0.06	0.88

Peak N°	Ex [a] (MeV)	Ex [b] (MeV±keV)	ℓ [a]	J^{π}	$(2J+1)C^2S$	$(d\sigma/d\Omega)_{CM}$ at 5° lab (mb/sr)
40	6.816	6.836 (12)	1	$(\frac{1}{2}, \frac{3}{2})^-$	0.13	2.2
41	6.910		(0)	$\frac{1}{2}^+$	0.02	0.28
42	6.981	6.986 (5)	3	$\frac{5}{2}^-$	0.14	0.24
43	7.026		1	$(\frac{1}{2}, \frac{3}{2})^-$	0.04	0.55
44 [d]	7.059	7.063 (5)	1	$\frac{1}{2}^-$	0.08	1.8
			4	$(\frac{9}{2}, \frac{7}{2})^+$	0.41	
45	7.151		ns			0.083
46	7.186		ns			0.061
47	7.253		1	$(\frac{1}{2}, \frac{3}{2})^-$	0.01	0.19
48	7.320		1	$(\frac{1}{2}, \frac{3}{2})^-$	0.06	0.98
49	7.342		3	$(\frac{5}{2}, \frac{7}{2})^-$	0.22	0.26
50	7.375		3	$(\frac{5}{2}, \frac{7}{2})^-$	0.18	0.28
51	7.421		3	$(\frac{5}{2}, \frac{7}{2})^-$	0.08	0.17
52	7.442		1	$(\frac{1}{2}, \frac{3}{2})^-$	0.01	0.17
53	7.483		3	$(\frac{5}{2}, \frac{7}{2})^-$	0.14	0.27
54	7.500		1	$(\frac{1}{2}, \frac{3}{2})^-$	0.03	0.44
55	7.529		4	$(\frac{9}{2}, \frac{7}{2})^+$	0.09	0.090
56	7.583		ns			0.080
57	7.653		1	$(\frac{1}{2}, \frac{3}{2})^-$	0.03	0.56
58	7.678		4	$(\frac{9}{2}, \frac{7}{2})^+$	0.14	0.130

Peak N°	Ex [a] (MeV)	Ex [b] (MeV±keV)	ℓ [a]	J^{π}	$(2J+1)C^2S$	$(d\sigma/d\Omega)_{CM}$ at 5° lab (mb/sr)
59	7.723		1	$(\frac{1}{2}, \frac{3}{2})^-$	0.05	0.88
60	7.746		4	$(\frac{9}{2}, \frac{7}{2})^+$	0.08	0.090
61	7.795		4	$(\frac{9}{2}, \frac{7}{2})^+$	0.10	0.11
62	7.832		1	$(\frac{1}{2}, \frac{3}{2})^-$	0.03	0.53
63	7.890		1	$(\frac{1}{2}, \frac{3}{2})^-$	0.18	3.2
64	7.940		ns			
65	7.998		1	$(\frac{1}{2}, \frac{3}{2})^-$	0.05	
66	8.029					
67	8.094		1	$(\frac{1}{2}, \frac{3}{2})^-$	0.08	1.4
68	8.147		1	$(\frac{1}{2}, \frac{3}{2})^-$	0.07	1.3
69	8.177		4	$(\frac{9}{2}, \frac{7}{2})^+$	0.07	0.11
70	8.200		1	$(\frac{1}{2}, \frac{3}{2})^-$	0.02	0.27
71	8.246					0.090
72	8.289		1	$(\frac{1}{2}, \frac{3}{2})^-$	0.02	0.41
73	8.330		3	$(\frac{5}{2}, \frac{7}{2})^-$	0.14	0.38
74	8.355		1	$(\frac{1}{2}, \frac{3}{2})^-$	0.04	0.65
75	8.434		1	$(\frac{1}{2}, \frac{3}{2})^-$	0.04	0.72
76	8.465		3	$(\frac{5}{2}, \frac{7}{2})^-$	0.08	0.22
77	8.625					0.22
78	8.693		2	$(\frac{5}{2}, \frac{3}{2})^+$	0.01	0.25

Peak N°	Ex [a] (MeV)	Ex [b] (MeV±keV)	ℓ [a]	J^{π}	$(2J+1)C^2S$	$(d\sigma/d\Omega)_{CM}$ at 5° lab (mb/sr)
79	8.721		1	$(\frac{1}{2}, \frac{3}{2})^-$	0.02	0.27
80[d]	8.751		1	$(\frac{1}{2}, \frac{3}{2})^-$	0.003	0.18
			+ (4)	$(\frac{9}{2}, \frac{7}{2})^+$	0.08	
81	8.781		1	$(\frac{1}{2}, \frac{3}{2})^-$	0.02	0.38
82	8.813		1	$(\frac{1}{2}, \frac{3}{2})^-$	0.04	0.70
83	8.848		1	$(\frac{1}{2}, \frac{3}{2})^-$	0.01	0.23
84	8.900		2	$(\frac{5}{2}, \frac{3}{2})^+$	0.04	0.70
85	8.929		3	$(\frac{5}{2}, \frac{7}{2})^-$	0.08	0.30
86	8.971		4	$(\frac{9}{2}, \frac{7}{2})^+$	0.04	-
87	9.008		2	$(\frac{5}{2}, \frac{3}{2})^+$	0.02	0.30
88	9.066		3	$(\frac{5}{2}, \frac{7}{2})^-$	0.03	0.12
89	9.117		2	$(\frac{5}{2}, \frac{3}{2})^+$	0.02	0.40
90	9.145		(1)	$(\frac{1}{2}, \frac{3}{2})^-$	0.01	0.24
91	9.185		(3)	$(\frac{5}{2}, \frac{7}{2})^-$	0.07	0.25
92	9.218		-	-	-	-
93	9.247		1	$(\frac{1}{2}, \frac{3}{2})^-$	0.05	-
94	9.295		1	$(\frac{1}{2}, \frac{3}{2})^-$	0.04	-
95	9.335					
96	9.385		1	$(\frac{1}{2}, \frac{3}{2})^-$	0.05	0.60
97	9.449		3	$(\frac{5}{2}, \frac{7}{2})^-$	0.11	0.37

Peak N°	Ex [a] (MeV)	Ex [b] (MeV±keV)	ℓ [a]	J^π	$(2J+1)C^2S$	$(d\sigma/d\Omega)_{CM}$ at 5° lab (mb/sr)
98	9.514		3	$(\frac{5}{2}, \frac{7}{2})^-$	0.08	0.28
99	9.575		1	$(\frac{1}{2}, \frac{3}{2})^-$	0.02	0.31
100	9.834		1	$(\frac{1}{2}, \frac{3}{2})^-$	0.05	0.70
101	9.675		1	$(\frac{1}{2}, \frac{3}{2})^-$	0.03	0.54
102	9.726		1	$(\frac{1}{2}, \frac{3}{2})^-$	0.08	-
103	9.790		1	$(\frac{1}{2}, \frac{3}{2})^-$	0.03	-
104	9.843		1	$(\frac{1}{2}, \frac{3}{2})^-$	0.09	-
105	9.873		1	$(\frac{1}{2}, \frac{3}{2})^-$	0.04	0.81
106	9.923		1	$(\frac{1}{2}, \frac{3}{2})^-$	0.08	1.2
107	9.956		3	$(\frac{5}{2}, \frac{7}{2})^-$	0.07	0.30
108	9.991		1	$(\frac{1}{2}, \frac{3}{2})^-$	0.01	0.16
109	10.059		1	$(\frac{1}{2}, \frac{3}{2})^-$	0.05	0.60
110	10.155		3	$(\frac{5}{2}, \frac{7}{2})^-$	0.04	0.17
111	10.212		1	$(\frac{1}{2}, \frac{3}{2})^-$	0.02	0.52
			+			
			(3)	$(\frac{5}{2}, \frac{7}{2})^-$	0.07	
112	10.413		1	$(\frac{1}{2}, \frac{3}{2})^-$	0.13	-
113	10.473		1	$(\frac{1}{2}, \frac{3}{2})^-$	0.07	-
114	10.617		1	$(\frac{1}{2}, \frac{3}{2})^-$	0.07	0.96
115	10.690		1	$(\frac{1}{2}, \frac{3}{2})^-$	0.07	0.84
116	10.787		(1)	$(\frac{1}{2}, \frac{3}{2})^-$	0.10	1.3

Peak N°	Ex [a] (MeV)	Ex [b] (MeV±keV)	ℓ [a]	J^π	$(2J+1)C^2S$	$(d\sigma/d\Omega)_{CM}$ at 5° lab (mb/sr)
117	10.870		(1)	$(\frac{1}{2}, \frac{3}{2})^-$	0.06	0.78
118	10.957		(1)	$(\frac{1}{2}, \frac{3}{2})^-$	0.07	0.80
119	11.021		(1)	$(\frac{1}{2}, \frac{3}{2})^-$	0.04	0.45
120	11.030		(1)	$(\frac{1}{2}, \frac{3}{2})^-$	0.04	0.55
121	11.138		(1)	$(\frac{1}{2}, \frac{3}{2})^-$	0.06	0.69
122	11.271		(1)	$(\frac{1}{2}, \frac{3}{2})^-$	0.17	1.9
123	11.425		2	$(\frac{5}{2}, \frac{3}{2})^+$	0.03	0.52
124	11.510		(3,4)	$(\frac{5}{2}, \frac{7}{2})^-$	0.08	0.40
125	11.558	11.5636(0.4)	1	$\frac{3}{2}^-$ [b]	0.53	5.6
126	11.665		1	$(\frac{1}{2}, \frac{3}{2})^-$	0.08	-
127	11.735			-	-	-
128	11.806			-	-	-
129	11.911		1	$(\frac{1}{2}, \frac{3}{2})^-$	0.09	0.48
130	11.976		1	$(\frac{1}{2}, \frac{3}{2})^-$	0.05	0.29
131	12.040		1	$(\frac{1}{2}, \frac{3}{2})^-$	0.07	0.48
132	12.098		(3,4)	$(\frac{5}{2}, \frac{7}{2})^-$	0.09	0.47
				$(\frac{9}{2}, \frac{7}{2})^+$	0.11	
133	12.160		(3,4)	$(\frac{5}{2}, \frac{7}{2})^-$	0.04	0.23
				$(\frac{9}{2}, \frac{7}{2})^+$	0.05	

Peak N°	Ex [a] (MeV)	Ex [b] (MeV±keV)	ℓ [a]	J^π	$(2J+1)C^2S$	$(d\sigma/d\Omega)_{CM}$ at 5° lab (mb/sr)
134	12.216		(3,4)	$(\frac{5}{2}, \frac{7}{2})^-$	0.03	0.19
				$(\frac{9}{2}, \frac{7}{2})^+$	0.04	
135	12.281		(3,4)	$(\frac{5}{2}, \frac{7}{2})^-$	0.03	0.21
				$(\frac{9}{2}, \frac{7}{2})^+$	0.04	
136	12.340		(3,4)	$(\frac{5}{2}, \frac{7}{2})^-$	0.03	0.16
				$(\frac{9}{2}, \frac{7}{2})^+$	0.04	
137	12.390		(3,4)	$(\frac{5}{2}, \frac{7}{2})^-$	0.03	0.15
				$(\frac{9}{2}, \frac{7}{2})^+$	0.03	
138	12.497		(1,2)	$(\frac{1}{2}, \frac{3}{2})^-$	0.17	0.53
				$(\frac{5}{2}, \frac{3}{2})^+$	0.04	
139	12.607		(3,4)	$(\frac{5}{2}, \frac{7}{2})^-$	0.05	0.25
				$(\frac{9}{2}, \frac{7}{2})^+$	0.06	
140	12.732		(3,4)	$(\frac{5}{2}, \frac{7}{2})^-$	0.10	0.51
				$(\frac{9}{2}, \frac{7}{2})^+$	0.11	
141	12.829		(3,4)	$(\frac{5}{2}, \frac{7}{2})^-$	0.05	0.27
				$(\frac{9}{2}, \frac{7}{2})^+$	0.06	
142	12.893		(3,4)	$(\frac{5}{2}, \frac{7}{2})^-$	0.03	0.13
				$(\frac{9}{2}, \frac{7}{2})^+$	0.03	
143	12.992		(3,4)	$(\frac{5}{2}, \frac{7}{2})^-$	0.11	0.62
				$(\frac{9}{2}, \frac{7}{2})^+$	0.12	

Peak N°	Ex [a] (MeV)	Ex [b] (MeV±keV)	ℓ [a]	J^π	$(2J+1)C^2S$	$(d\sigma/d\Omega)$ at 5° lab (mb/sr)
144	13.119		(3,4)	$(\frac{5}{2}, \frac{7}{2})^-$	0.12	0.74
				$(\frac{9}{2}, \frac{7}{2})^+$	0.15	
145	13.204		(3,4)	$(\frac{5}{2}, \frac{7}{2})^-$	0.04	0.20
				$(\frac{9}{2}, \frac{7}{2})^+$	0.04	
146	13.308		(3,4)	$(\frac{5}{2}, \frac{7}{2})^-$	0.08	0.56
				$(\frac{9}{2}, \frac{7}{2})^+$	0.09	
147	13.358		(3,4)	$(\frac{5}{2}, \frac{7}{2})^-$	0.03	0.14
				$(\frac{9}{2}, \frac{7}{2})^+$	0.03	
148	13 412		(3,4)	$(\frac{5}{2}, \frac{7}{2})^-$	0.05	0.28
				$(\frac{9}{2}, \frac{7}{2})^+$	0.06	
149	13.487	13.487(30)	(1)	$(\frac{1}{2}^-)$	0.10	0.40
150	13.557		1	$(\frac{1}{2})^-$	0.09	0.35
151	13.593		(1)	$(\frac{1}{2}^-)$	0.05	0.20
152	15.094	15.113(10)	3	$(\frac{5}{2}^-)$ [b]	0.06	0.40
153	15.584	15.560(5)	3	$\frac{5}{2}^-$ [e]	0.32	2.3
154	15.630	15.619(5)	4	$\frac{9}{2}^+$ [b]	0.27	1.8
155	16.900	16.991(10)	4	$\frac{9}{2}^+$ [b]	0.06	0.35
156	18.000		(3,4)		0.08	0.35
					0.08	

a) Present work : Excitation energies are given with an uncertainty estimated about 8 keV for levels below 8 MeV, 20 keV from 8 to 12 MeV, 40 keV from 12 to 16 MeV, and 80 keV above. Peaks with non-stripping angular distributions are labelled "n s"

b) réf. [1] c) réf. [16] d) doublet of levels e) réf. [2]

Table 2 : Optical-model potentials[a] used in the DWBA calculations.

Particle	V_o (MeV)	r_o (fm)	a_o (fm)	W (MeV)	W_D (MeV)	r'_o (fm)	a'_o (fm)	r_{oc} (fm)
p	U_o	1.25	0.65					
^{3}He[b]	155.9	1.20	0.72	40.7		1.40	0.88	1.3
d[c]	V_d[d]	1.15	0.81		W_d[d]	1.34	0.68	1.15

c) The potentials for ^{3}He and d were of the form :

$V(r) = V_c - V_o f(x) - i(W f(x') - 4 W_D \frac{d}{d_{x'}} f(x')$, where $f(x_i) = (1+e^{x_i})^{-1}$

with $x_i = (r-r_i A^{1/3})/a_i$ and V_c is the Coulomb potential. The form factors are computed with a binding potential :

$U(r) = -U_o[f(x) - \lambda \frac{\vec{L}\vec{S}}{45.2} \frac{d}{dx} f(x)]$ with $\lambda = 25$

b) réf. [8]

c) réf. [9]

d) $V_d = 81.0 - 0.22\ E + 2.0\ (Z/A^{1/3})$; $W_d = 14.4 + 0.24\ E$; where E is the incident energy in MeV.

Table 3 :

Comparison of spectroscopic strengths determined in the $^{48}Ca(^{3}He,d)^{49}Sc$ reaction at different energies.

E_x (MeV)	ℓ	$(2J+1)C^2S$				
		25 MeV present data	12 MeV réf. 13)	18 MeV ref. 14)	22 MeV ref. 15)	30.2 MeV ref. 12)
0.0	3	6.72	8.0	7.83	7.23	8.0
2.23	0	0.03	-	-	-	0.12
2.37	2	0.05	-	-	-	0.25
3.08	1	2.08	2.4	2.51	2.41	2.16
3.81	3	0.53	0.6	0.58	0.90	0.83
4.07	3	0.98	0.8	0.77	1.26	1.18
4.33	3	0.44	-	0.38	0.54	0.63
4.49	1	1.04	1.1	1.34	-	0.86
4.74	3	0.70	0.4	0.67	0.90	1.09
5.02	1	0.19	0.21	0.21	-	0.23
5.08	3	1.99	1.4	1.82	2.22	2.43
5.38	3	0.81	0.6	0.68	0.84	1.00
5.66	1	0.39	0.47	0.46	0.54	0.46
5.81	1	0.08	0.12	0.13	0.16	0.16
6.41	3	0.27	-	-	-	0.16
6.53	1 + 4	0.03 + 0.20	0.05 -	0.05 -	- -	- -
6.72	1	0.06	0.06	0.05	-	-
6.82	1	0.13	0.17	0.20	-	-
6.91	0		0.12			
7.06	1 + 4	0.08 + 0.41	0.15 a) -	-	-	- (0.6) b)

a) Level located at 7081 ± 12 keV in réf. 13)

b) Level located at 7.15 MeV in réf. 12)

Table 4 : Spectroscopic factors of analog states in ^{49}Sc, as deduced from (^3He,d) and (p,p) measurement and comparison with those found in the (d,p) reaction for parent states in ^{49}Ca.

Analog state in ^{49}Sc							Parent state in ^{49}Ca		
E_x a) (MeV)	E_x b) (MeV)	$E_x - E_o$ a) (MeV)	ℓ_j b)	$S(^3He,d)$ a)	$S(^3He,dp)$ c)	$S_{p,p}$ d)	E_x b) (MeV)	ℓ_j b)	$S(d,p)$ e)
11.56 ± 0.02	11.563 ± 0.004	0	p3/2	1.19	0.64 ± 0.08	0.64 ± 0.07	0	p3/2	0.93
13.54 ± 0.04 f)	13.48 ± 0.03	1.98	(p1/2)	1.08 g)		1.24 ± 0.27	2.02	p1/2	0.98
15.09 ± 0.04	15.11 ± 0.01	3.53	f5/2	0.09		0.11 ± 0.03	3.59	f5/2	0.14
15.58 ± 0.04	15.560 ± 0.005	4.02	f5/2	0.48	0.60 ± 0.15	0.64 ± 0.16	3.86	f5/2	0.80
15.63 ± 0.04	15.61 ± 0.005	4.07	g9/2	0.24	0.47 ± 0.20	0.30 ± 0.15	3.99	g9/2	0.30
16.90 ± 0.08	16.99	5.34	g9/2	0.05		0.06 ± 0.01	5.39	g9/2	0.06
(18.00 ± 0.08)	18.15	6.44	d5/2				≈6.7		

a) Present work. E_o is the excitation energy of the analog of the ^{49}Ca ground state. S is obtained by multiplying the C^2S value by $(2T_o+1)$, with T_o isospin of the ^{48}Ca ground state .

b) réf. [1], c) réf. [2], d) From réf. [18] for the p3/2 and p1/2 states, and from réf. [19] for higher lying analog states. e) réf. [17].

f) Energy centroid of the three observed $\ell = 1$ levels at 13.49, 13.56 and 13.59 MeV.

g) Sum of the spectroscopic factors for the three $\ell = 1$ levels.

Table 5 : Comparison of summed experimental transition strengths $\Sigma(2J+1)C^2S$ with the shell-model (SM) sum-rule limit and centroid energies of proton states in ^{49}Sc [a].

Single particle orbital	$\Sigma(2J+1)C^2S$ $T_<$ exp		$\Sigma(2J+1)C^2S$ $T_<$ S.M.		$\Sigma(2J+1)C^2S$ $T_>$ exp	$\Sigma(2J+1)C^2S$ $T_>$ S.M.	$\overline{E}_p(T_<)$ (MeV)	$\overline{E}_p(T_>)$ (MeV)
1f7/2	7.4[b]	13.8	8	13.3	-	0	0.5[b]	-
1f5/2	6.4[b]		5.3		0.38	0.66	5.7[b]	15.5
2p3/2	2.1[c] or 3.6[d]	5.9	3.6	5.4	0.53	0.44	3.8[b] or 4.5[c]	11.6
2p1/2	3.8[c] or 2.3[d]		1.8		0.24	0.22	8.0[b] or 8.5[c]	13.5
1g9/2	2.4		8.9		0.33	1.11	10.1	15.9

a) See discussion in the text.

b) All $\ell = 3$ levels, except previously known $7/2^-$ levels, are assumed to have $J^\pi = 5/2^-$.

c) All $\ell = 1$ levels, except previously known $3/2^-$ levels, are assumed to have $J^\pi = 1/2^-$

d) All $\ell = 1$ levels below 8 MeV excitation energy, except previously known $1/2^-$ levels, are assumed to have $J^\pi = 3/2^-$.

Figure Captions

Fig. 1a) Deuteron spectrum from the $^{48}Ca(^{3}He,d)^{49}Sc$ reaction at 5°lab, observed in the focal plane of the split-pole spectrometer for the 0.11 MeV region of excitation energies. The numbers on the top of the peaks refer to ^{49}Sc levels and are listed in table 1.

Fig. 1b) Same as fig. 1a, but for the 11 - 18 MeV region of excitation energy in ^{49}Sc.

Fig. 2) Examples of angular distributions for levels excited with an $\ell = 1$ transfer.

Fig. 3) Examples of angular distributions for levels excited with an $\ell = 3$ transfer.

Fig. 4) Examples of angular distributions for levels excited with an $\ell = 0$, $\ell = 2$ or $\ell = 4$ transfer (see text).

Fig. 5) Distribution of spectroscopic strengths from the $^{48}Ca(^{3}He,d)^{49}Sc$ reaction. The $(2J+1)C^2S$ values for each ℓ-transitions are represented by the length of the vertical bars.

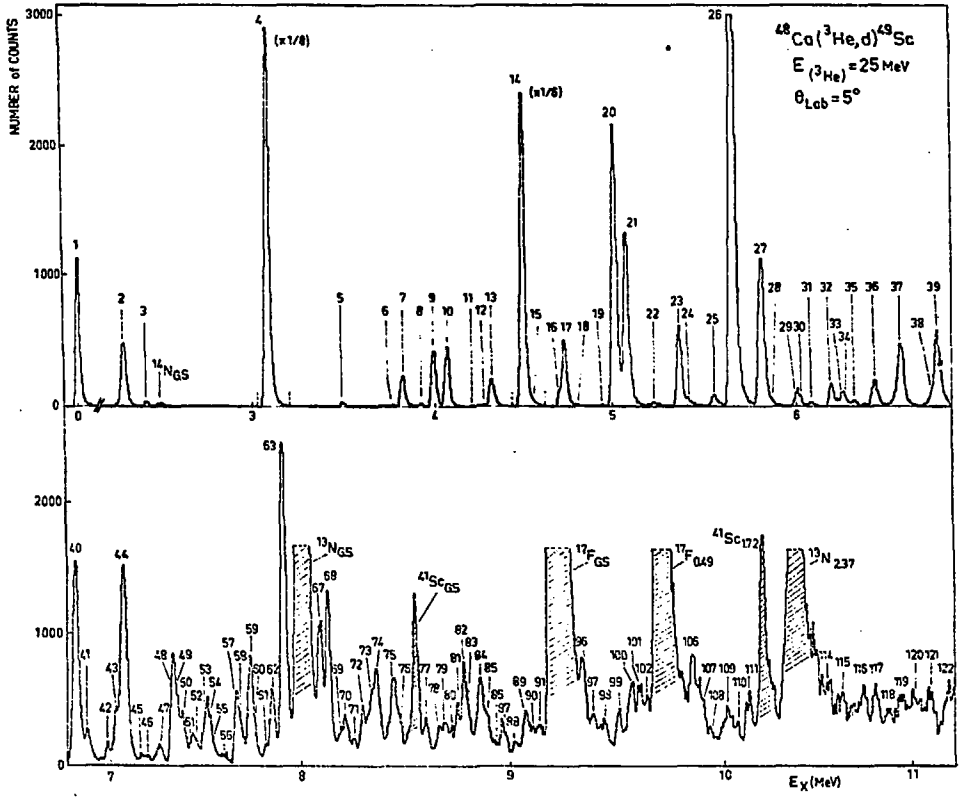
NUMBER of COUNTS
$^{48}Ca(^{3}He,d)^{49}Sc$
$E_{(^{3}He)}=25$ MeV
$\theta_{Lab}=5°$
(x1/8)
(x1/8)
$^{14}N_{GS}$
$^{13}N_{GS}$
$^{41}Sc_{GS}$
$^{17}F_{GS}$
$^{17}F_{0.49}$
$^{41}Sc_{1.72}$
$^{13}N_{2.37}$
E_X(MeV)

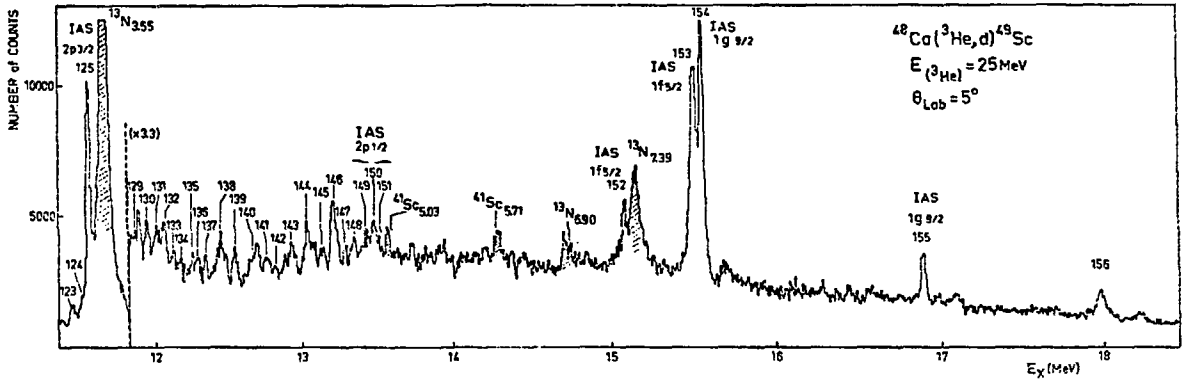
NUMBER of COUNTS
10000
5000
IAS
2p3/2
125
13N3.55
(x3.3)
IAS
2p1/2
150
IAS
1f5/2
153
IAS
1g 9/2
154
IAS
1f5/2
152
13N7.39
41Sc5.03
41Sc5.71
13N6.90
IAS
1g 9/2
155
156
124
123
129
130
131
132
133
134
135
136
137
138
139
140
141
142
143
144
145
146
147
148
149
151
12
13
14
15
16
17
18
Ex(MeV)
48Ca(3He,d)49Sc
E(3He) = 25MeV
θLab = 5°

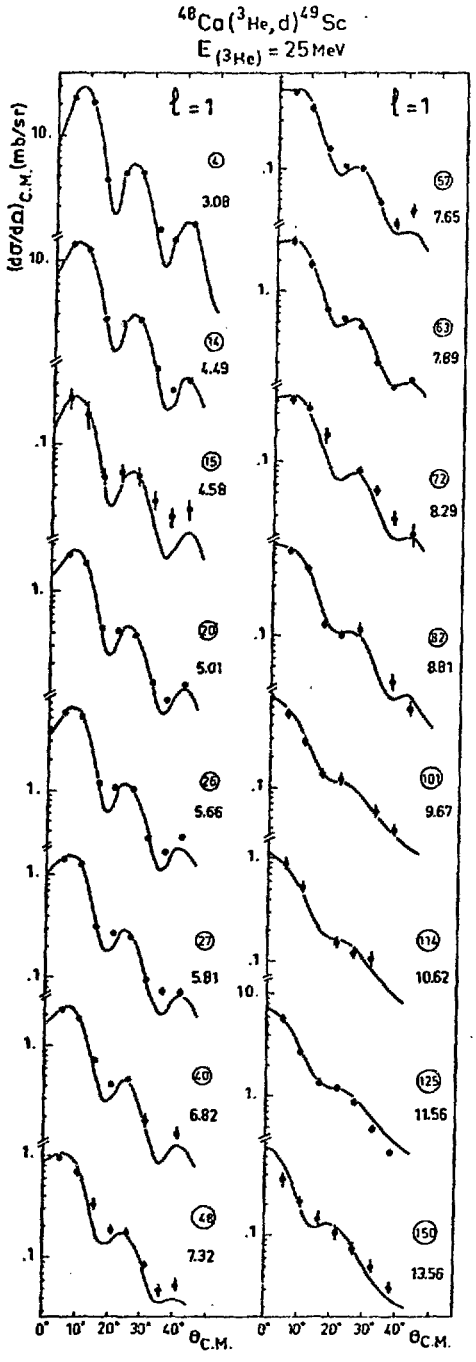
$^{48}Ca(^{3}He,d)^{49}Sc$
$E_{(^{3}He)} = 25\,MeV$
$(d\sigma/d\Omega)_{C.M.}$ (mb/sr)
$\ell = 1$
$\ell = 1$
4
3.08
14
4.49
15
4.58
20
5.01
26
5.66
27
5.81
40
6.82
48
7.32
57
7.65
63
7.89
72
8.29
82
8.81
101
9.67
114
10.62
125
11.56
150
13.56
$\theta_{C.M.}$
$\theta_{C.M.}$

Fig. 9

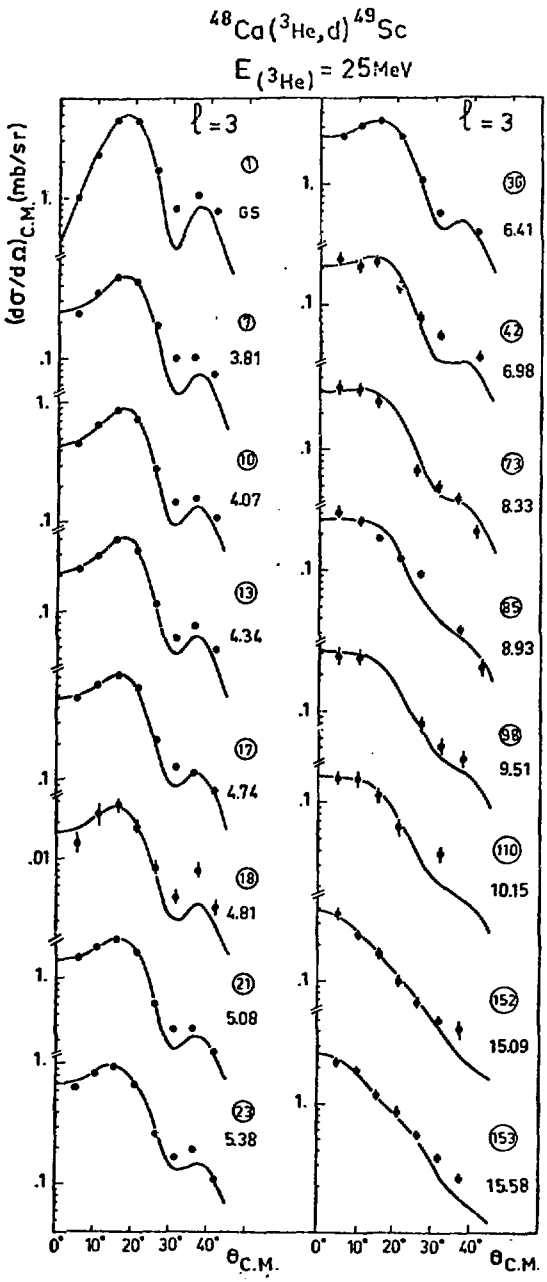
$^{48}Ca(^{3}He,d)^{49}Sc$
$E_{(^{3}He)} = 25MeV$
$(d\sigma/d\Omega)_{C.M.}$ (mb/sr)
$\ell = 3$
$\ell = 3$
① GS
⑦ 3.81
⑩ 4.07
⑬ 4.34
⑰ 4.74
⑱ 4.81
㉑ 5.08
㉓ 5.38
㉚ 6.41
㊷ 6.98
㊸ 8.33
㊽ 8.93
㊾ 9.51
⑪⓪ 10.15
⑮② 15.09
⑮③ 15.58
0° 10° 20° 30° 40° $\theta_{C.M.}$
0° 10° 20° 30° 40° $\theta_{C.M.}$

fig. 3

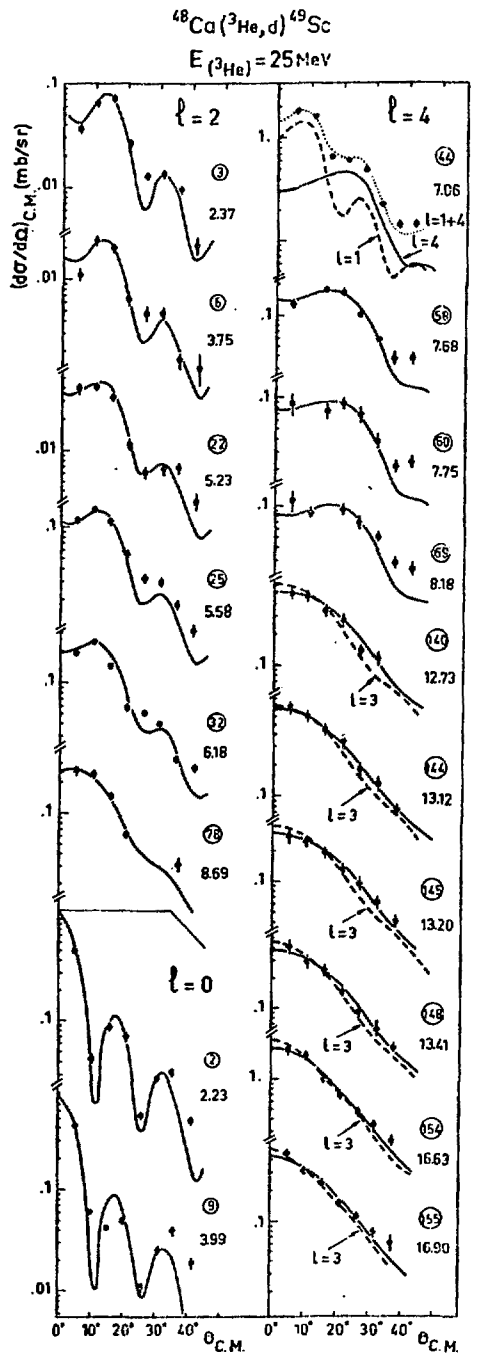
$^{48}Ca(^3He,d)^{49}Sc$
$E_{(^3He)} = 25$ MeV
$(d\sigma/d\Omega)_{C.M.}$ (mb/sr)
$\theta_{C.M.}$
$\ell = 2$
$\ell = 4$
$\ell = 0$
$\ell = 1$
$\ell = 3$
$\ell = 1+4$
3 2.37
6 3.75
22 5.23
25 5.58
32 6.18
38 8.69
7 2.23
9 3.99
44 7.06
58 7.68
60 7.75
69 8.18
140 12.73
144 13.12
145 13.20
148 13.41
154 16.63
155 16.90

Fig 4

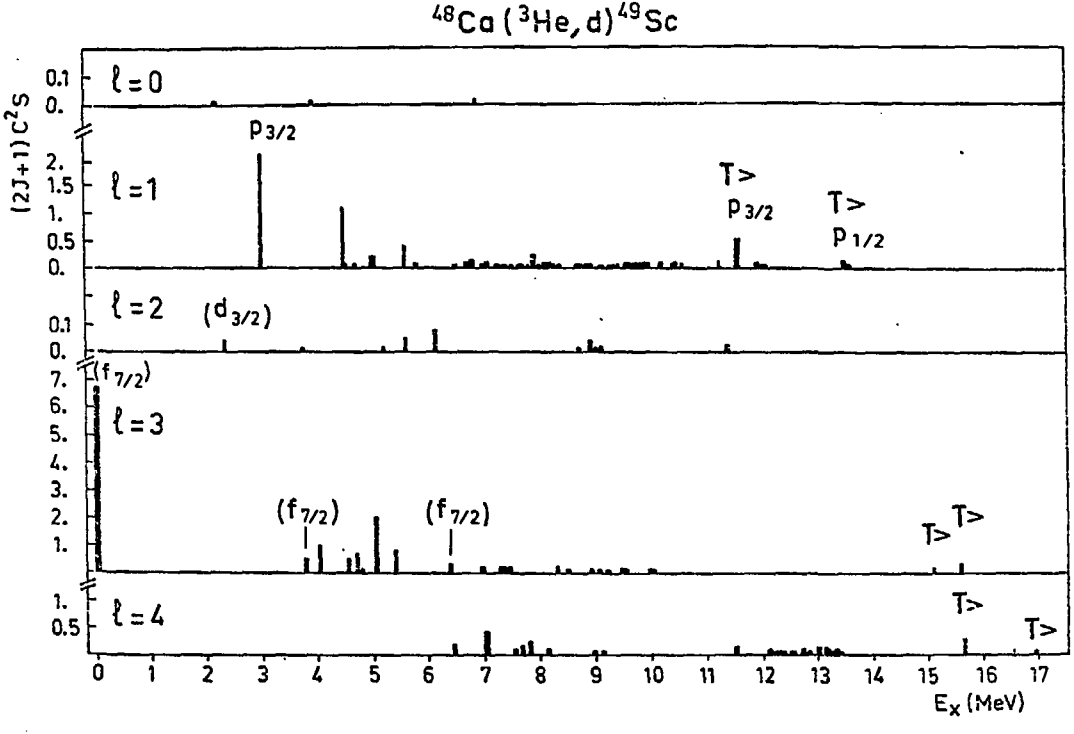
$^{48}Ca(^{3}He,d)^{49}Sc$
$(2J+1)C^2S$
ℓ=0
ℓ=1
ℓ=2
ℓ=3
ℓ=4
$p_{3/2}$
T> $p_{3/2}$
T> $p_{1/2}$
$(d_{3/2})$
$(f_{7/2})$
$(f_{7/2})$
$(f_{7/2})$
T>
T>
T>
T>
E_x (MeV)

Fig 5.